Gynecologic Oncology 153 (2019) 416–424

Contents lists available at ScienceDirect

Gynecologic Oncology

journal homepage: www.elsevier.com/locate/ygyno

ERCC1-XPF deficiency is a predictor of olaparib induced synthetic lethality and platinum sensitivity in epithelial ovarian cancers

Katia A. Mesquita [a], Muslim Alabdullah [a,b], Michaela Griffin [a], Michael S. Toss [b], Tarek M.A. Abdel Fatah [c], Adel Alblihy [a], Paul Moseley [c], Stephen Y.T. Chan [c], Emad A. Rakha [b], Srinivasan Madhusudan [a,c,*]

[a] Translational Oncology, Division of Cancer and Stem Cells, School of Medicine, University of Nottingham, Nottingham University Hospitals, Nottingham NG5 1PB, UK
[b] Department of Pathology, Division of Cancer and Stem Cells, School of Medicine, University of Nottingham, Nottingham NG51PB, UK
[c] Department of Oncology, Nottingham University Hospitals, City Hospital Campus, Nottingham NG5 1PB, UK

HIGHLIGHTS

- PARP inhibitor therapy improves progression free survival in platinum sensitive ovarian cancers.
- Robust biomarker to predict benefit from PARP inhibitor therapy in sporadic tumors is yet to be established.
- Here we show that ERCC1-XPF deficiency predicts platinum sensitivity.
- ERCC1 or XPF deficient ovarian cancer cells are sensitive to PARP inhibitor Olaparib through synthetic lethality.

ARTICLE INFO

Article history:
Received 8 October 2018
Received in revised form 24 January 2019
Accepted 17 February 2019
Available online 21 February 2019

Keywords:
Ovarian cancer
DNA repair
ERCC1
XPF: PARP
Biomarker
Predictive
Synthetic lethality

ABSTRACT

Purpose. PARP inhibitor maintenance therapy in platinum sensitive sporadic ovarian cancers improves progression free survival. However, biomarker for synthetic lethality in platinum sensitive sporadic disease is yet to be defined. ERCC1-XPF heterodimer is a key player in nucleotide excision repair (NER) involved in the repair of platinum induced DNA damage. In the current study, we tested whether ERCC1-XPF deficiency would predict synthetic lethality to the PARP inhibitor Olaparib and platinum sensitivity in ovarian cancers.

Methods. ERCC1, XPF and PARP1 protein expression was evaluated in tumors from a cohort of 331 patients treated at Nottingham University Hospitals and correlated to clinicopathological features and survival. Pre-clinically, ERCC1 and XPF was depleted in A2780 (platinum sensitive) and A2780cis (platinum resistant) ovarian cancer cell lines and tested for platinum sensitivity as well as for Olaparib induced synthetic lethality.

Results. Low ERCC1 was significantly associated with improved progression free survival (PFS) in patients with ovarian cancers in univariate ($p = 0.001$) and multivariate ($p = 0.002$) analysis. In addition, low ERCC1/low XPF ($p = 0.003$) or low ERCC1/low PARP1 ($p = 0.0001$) tumors was also linked to better PFS compared to high ERCC1/high XPF or high ERCC1/high PARP1 tumors. Pre-clinically, ERCC1 or XPF depletion not only increased platinum sensitivity but also increased toxicity to Olaparib therapy. Increased sensitivity was associated with DNA double strand breaks (DSBs) accumulation, cell cycle arrest and increased apoptosis.

Conclusion. The data provide evidence that low ERCC1 is not only a predictor of platinum sensitivity but is also a promising biomarker for Olaparib induced synthetic lethality in ovarian cancers.

1. Introduction

In platinum sensitive sporadic epithelial ovarian cancers, PARP inhibitor (Niraparib, Olaparib and Rucaparib) maintenance therapy was recently shown to substantially improve progression free survival in patients [1–3]. However, biomarker of response to Olaparib or Niraparib or Rucaparib therapy in platinum sensitive disease is yet to be clearly defined. Moreover, platinum resistance is a formidable clinical problem in ovarian cancers.

Platinating agents such as cisplatin, carboplatin are frequently used in ovarian cancer therapy. The cytotoxicity of platinum drugs is directly related to their ability to interact with DNA and form intra-strand crosslink DNA adducts. If the DNA damaging adducts are not repaired, the cells accumulate such toxic lesions which lead to cell cycle arrest and ultimately cell death [4]. Platinum induced DNA damage is

* Corresponding author at: Translational Oncology, Division of Cancer and Stem Cells, School of Medicine, University of Nottingham, Nottingham University Hospitals, Nottingham NG51PB, UK.
E-mail address: srinivasan.madhusudan@nottingham.ac.uk (S. Madhusudan).

https://doi.org/10.1016/j.ygyno.2019.02.014
0090-8258/

processed through the DNA repair machinery in cancer cells. The nucleotide excision repair (NER) is the critical DNA repair pathway that effectively repairs platinum induced DNA damage in cells. NER is a highly conserved, versatile and robust. Increased NER capacity will result in the repair of platinum induced DNA damage and therefore is an important predictor of platinum resistance in cancer cells [5]. NER is a complex pathway requiring several proteins and their interacting partners. Although complex, two sub-pathways of NER has been described; the transcription-coupled nucleotide excision repair (TC-NER) pathway that targets lesions specifically in the transcribed strand of expressed genes and the global genome nucleotide excision repair (GG-NER) pathway that deals with lesions in the rest of the genome. Although these NER sub-pathways are complex, basic steps in GG-NER include; DNA damage recognition [by XPC-HR23B complex], lesion demarcation and verification by TFIIH complex [Cdk7, Cyclin H, MAT1, XPB, XPD, p34, p44, p52 and p62], assembly of a pre-incision complex [RPA, XPA and XPG], DNA opening by XPB and XPD helicases, dual incision [by ERCC1-XPF and XPG endonucleases], release of the excised oligomer and finally repair synthesis to fill in the resulting gap [RPA, RFC, PCNA, Pol δ/ε), and ligation (ligase I)] [6,7]. In TC-NER, translocating RNA polymerase II detects lesions in the template. A role for ERCC8 (CSA) and ERCC6 (CSB) has also been suggested in DNA damage recognition in TC-NER. Subsequent steps in TC-NER are similar to GC-NER.

XPF and ERCC1 proteins are critical players in NER. XPF endonuclease (also known as ERCC4) associates with its non-catalytic partner ERCC1. The ERCC1-XPF heterodimer cleaves and facilitates the removal of bulky lesions such as those induced by platinum chemotherapy [8,9]. In addition ERCC1-XPF heterodimer also has essential roles in other DNA repair pathways such as DNA recombinational repair and interstrand crosslink repair [10,11]. Our hypothesis is that high ERCC1-XPF will determine platinum resistance in ovarian cancers. ERCC1 or XPF deficient ovarian cancer will not only be platinum sensitive but such cells will also be sensitive to the PARP inhibitor Olaparib.

2. Materials and methods

2.1. Clinical study

2.1.1. ERCC1, XPF and PARP1 level in ovarian cancers

Investigation of the expression of ERCC1, XPF and PARP1 in ovarian epithelial cancer was carried out on tissue microarrays of 331 consecutive ovarian epithelial cancer cases treated at NUH between 1997 and 2010. The characteristics of this cohort are summarized in Supplementary Table S1. None of the tumors were BRCA deficient.

2.1.2. Tissue microarrays (TMAs) and immunohistochemistry (IHC) evaluation

Tumors were arrayed in tissue microarrays (TMAs) constructed with 2 replicate 0.6 mm cores from the tumors. Immunohistochemical staining was performed using the Thermofisher Scientific Shandon Sequenza chamber system (REF: 72110017), in combination with the Novolink Max Polymer Detection System (RE7280-K: 1250 tests), and the Leica Bond Primary Antibody Diluent (AR9352), each used according to the manufacturer's instructions (Leica Microsystems). The tissue slides were deparaffinised with xylene and then rehydrated through five decreasing concentrations of alcohol (100%, 90%, 70%, 50% and 30%) for 2 min each. Pre-treatment antigen retrieval was performed on the TMA sections using sodium citrate buffer (pH 6.0) and heated for 20 min at 95 °C in a microwave (Whirpool JT359 Jet Chef 1000W). A set of slides were incubated with the primary anti-ERCC1 mouse monoclonal antibody [clone 4F9 (catalogue number: M3648), Dako Ltd., UK], at a dilution of 1:50 incubated for 60 min. For XPF (NB100-60689, Novus Biologicals) the concentration of the antibody was 1:200 and the incubation period was 18 h on a cold room. Regarding PARP1 (7D3-6, BD Pharmigen), TMA sections were stained with purified mouse anti-human PARP1 antibody (1:600) for 60 min incubation in room temperature. Negative (by omission of the primary antibody and IgG-matched serum) and positive controls were included in each run.

Whole field inspection of the core was scored and intensities of nuclear staining were grouped as follows: 0 = no staining, 1 = weak staining, 2 = moderate staining, 3 = strong staining. The percentage of each category was estimated (0–100%). Histochemical score (H-score) (range 0–300) was calculated by multiplying intensity of staining and percentage staining. A median H score of ≥100 and >0 was utilised as the cut-off for high ERCC1 nuclear and cytoplasmic expression respectively. For PARP1 nuclear expression, a median score of ≥80 was used as the optimal cut-off for high expression. Regarding XPF, a median H score of >0 and >100 was taken as the cut-off for high XPF nuclear and cytoplasmic expression respectively. Not all cores within the TMA were suitable for IHC analysis as some cores were missing or lacked tumor.

2.1.3. Statistical analysis

This was performed using SPSS v 22 (Chicago, IL, USA) for Windows. Association with clinical and pathological parameters using categorised data was examined using Chi-squared test. All tests were 2-tailed. Survival rates were determined using Kaplan–Meier method and compared by the log-rank test. All analyses were conducted using Statistical Package for the Social Sciences (SPSS, version 22, Chicago, IL, USA) software for windows. *P* value of <0.05 was identified as statistically significant. This work was approved by the Nottingham Research Ethics Committee.

2.1.4. ERCC1 transcript in ovarian cancers

ERCC1 mRNA was evaluated in a publically available online gene expression dataset of 1287 ovarian cancer patients treated with platinum based chemotherapy from 8 previously published studies and available at 'http://kmplot.com/analysis/index.php?p=service&cancer=ovar'.

2.2. Pre-clinical study

2.2.1. Cell culture

A2780 and A2780cis human ovarian cancer cell lines were purchased from Sigma Aldrich (Gillingham, UK). PEO4 was purchased from American Type Culture Collection (ATCC, Manassas, USA). A2780, A2780cis and PEO4 cells were cultured in RPMI (R8758, Merck, UK) with 10% FBS (F4135, Merck, UK), 1% Penicillin-Streptomycin (P4333, Merck, UK). All cell lines were maintained in a humidified incubator at 37 °C in a 5% CO_2 atmosphere.

2.2.2. Clonogenic assays

In the sensitivity assay (Clonogenic) 32 cells/cm^2 were seeded in 6-well plates and left at 37 °C in a 5% CO_2 atmosphere. Cisplatin (provided by the chemotherapy department of Nottingham University Hospitals, Nottingham, UK) was added at the indicated concentrations and the plates were left at 37 °C in a 5% CO_2 atmosphere for 14 days. Later the plates were washed with PBS, fixed and stained and colonies were counted.

2.2.3. Nuclear and cytoplasmic extract

Cells were harvest by trypsinization, washed with PBS and centrifuge at 1000 ×*g* for 5 min. Nuclear and cytoplasmic lysates were extracted using the NE-PER™ Nuclear and Cytoplasmic Extraction Reagents Thermofisher Scientific, UK. Cell number was counted and re-suspended in the appropriate solutions volumes according to the manufacturer's instructions. Any supernatant was carefully removed to ensure a completely dry pellet and ice cold CER I was added to the pellet. The tube was vortexed on the highest setting for 15 s and the sample was then incubated on ice for 10 min. Following this, ice cold CER II was added to the suspension and vortexed at the highest speed for 5 s. Samples were then centrifuged at 13,000 rpm (>16,000*g*) for 15 min. After this the supernatant (cytoplasmic extract) was collected and stored at −80 °C. The remaining pellet was re-suspended on NER

reagent and vortexed on the highest setting for 15 s. Vortexing was repeated every 10 min for 40 min, with samples being incubated on ice between vortexing. Samples were then centrifuged at 13,000 rpm (>16,000*g*) for 20 min and the supernatant (nuclear extract) was collected and stored at −80 °C.

2.2.4. ERCC1 or XPF knockdown using siRNAs

Cells were transfected with 20 nM of either mERCC1 siRNA oligonucleotide AM16708, Ambion, Thermofisher Scientific, id: construct 1-146876 and construct 2-146877) or mXPF siRNA oligonucleotide (AM16708, Ambion, Thermofisher Scientific, id: construct 1-146633 and construct 2-146632) or scrambled siRNA control (4390843, Thermofisher). Briefly, 24 h before the transfection, cells were seeded at a density of 8×10^3 cells/cm^2, approximately 50–60% confluency. Transfection process was made using Lipofectamine 3000 transfection reagent (L3000015, Invitrogen) according to the manufacturer's instructions. ERCC1 and XPF silencing was confirmed by western blot.

2.2.5. Western Blot analysis

Cells were harvested and lysed in RIPA buffer (R0278, Sigma) with the addition of protease inhibitor cocktail (P8348, Sigma), phosphatase inhibitor cocktail 2 (P5726, Sigma) and phosphatase inhibitor cocktail 3 (P0044, Sigma) and stored at −20 °C. Protein was quantified using BCA Protein Assay kit (23225, Thermofisher S). The following antibodies were used: ERCC1 (1:2000, M3648, DAKO), XPF (1:500, NB100-60689, Novus Biologicals), β-Tubulin (1:1000, ab6046), YY1 (1:1000, ab109228), GADPH (1:1000, ab9485), PARP1 (1:1000, 7D3-6, BD Pharmigen), p53 (phospho S46) [EP42Y] (1:1000, ab76242), p53 (phospho S392) [EP155Y] (1:1000, ab33889) and p53 (acetyl K382) [EPR358(2)] (1:1000, ab75754). Infrared dye-labelled secondary antibodies (LiCor) [IRDye 800CW Donkey Anti-Rabbit IgG and IRDye 680CW Donkey Anti-Mouse IgG] were incubated at a dilution of 1:10,000 for 1 h. Membranes were scanned and density of each band was calculated in a LiCor Odyssey machine (700 and 800 nm) to determine protein levels. β-Tubulin was used as a loading control for the whole cell lysates. GADPH and YYI were used as loading controls to cytoplasmic and nuclear fractions, respectively. Bar charts show means of optical density (O.D.) ± S.D. and all data is representative of at least three independent experiments.

2.2.6. Functional studies

1.05×10^4 cells/cm^2 were seeded in 6-well plates and left overnight at 37 °C in a 5% CO_2 atmosphere. Next, Cisplatin or Olaparib (kindly provided by AstraZeneca Pharmaceuticals) were added to cells and incubated for 24 h and 48 h at 37 °C in a 5% CO_2 atmosphere. Cells were collected by trypsinization, washed with ice cold PBS and fixed in 70% ethanol for 1 h at −20 °C. After removal of the fixative solution by centrifugation, For DNA double strand break analysis, cells were stained with 2 μg/ml of phospho-Histone (γH2AX) Ser139 (16202A, Millipore, UK) to detect DSBs. For cell cycle analysis, Cells were treated with 20 μg/ml RNase A (12091021, Invitrogen) and then 10 μg/ml Propidium Iodide (P4170, Sigma Aldrich) was added to determine the cell cycle distribution. The samples were analysed on a Beckman-Coulter FC500 flow cytometer using a 488 nm laser for excitation and emission data for PI collected using a 620 nm bandpass filter (FL3) and a 525 nm bandpass filter (FL1) for FITC-anti-phospho-Histone H2A.X. For the Apoptosis assay, cells were analysed using Annexin V detection kit (556547, BD Biosciences). Briefly, cells were trypsinized, washed with PBS and the cellular pellet was re-suspended in Anexin Binding Buffer (1×). Following, 2.5 μl of FITC Anexin V and 2.5 μl of Propidium Iodide were added to the cells. After incubation 300 μl of Anexin Binding Buffer (1×) was added to each tube. All the samples were analysed on a Beckman-Coulter FC500 flow cytometer. The percentage of apoptotic cells was determined (late apoptotic = FITC-Annexin V positive, PI positive early apoptotic = FITC-Annexin V positive, PI negative; live cells = FITC-Annexin V negative, PI negative) and compared for untreated and treated samples. Graphical representation and statistical analysis was performed in GraphPad Prism 7 (GraphPad, La Jolla, USA). All data is representative of at least three independent experiments.

2.2.7. Statistical analysis

Data are means values ± SD from at least three separate experiments. In statistical analysis to compare A2780 and A2780cis the Student's *t*-test was used. For comparisons of more than two groups an ANOVA one-way (variances analyses) with no matched pairs but with multiple comparisons test was used. A two-way ANOVA was used to analyses two variables (e.g. time and drug effect), with same considerations previously explained. The multiple comparisons were made using Bonferroni post-hoc test or (Holm-) Sidak's test using selected comparisons.

3. Results

3.1. ERCC1 and XPF in ovarian cancers

A total of 235 tumors were suitable for ERCC1 analysis (Fig. 1A2). 114/235 (48.5%) tumors showed reduced/absent expression of ERCC1 level (ERCC-) whereas 121/235 (51.5%) of tumors had high nuclear ERCC1 expression (ERCC1+) (Supplementary Table S2). High ERCC1 level was significantly associated with serous type carcinomas ($p = 0.000053$), higher FIGO stage at presentation ($p = 0.049$) and higher tumor grade ($p = 0.047$) (Supplementary Table S2). High ERCC1 level was associated with poor progression free survival (PFS) ($p = 0.001$) (Fig. 1B) and overall survival (OS) ($p = 0.05$) (Fig. 1C). A total of 229 tumors were suitable for XPF analysis (Fig. 1A3). We did not observe any significant associations between XPF and clinicopathological variables (Supplementary Table S3) or survival (Supplementary Fig. S1A and B). When ERCC1 and XPF were combined together ($n = 206$), nuclear ERCC1+/XPF- tumors were more likely to be serous cystadenocarcinomas ($p = 0.005$) (Supplementary Table S4). Patients with nuclear ERCC1-/XPF- tumors had a favorable PFS (Fig. 1D) ($p = 0.003$) and OS (Fig. 1E) ($p = 0.048$) compared to ERCC1+/XPF- tumors.

3.2. ERCC1-PARP1 co-expression and ovarian cancers

A previous study in non-small cell lung cancer (NSCLC) suggested that low ERCC1/low PARP1 tumors were more likely to benefit from platinum based chemotherapy [12]. In addition, PARP1 inhibition has also been shown to improve platinum sensitivity in low ERCC1 NSCLCs [13]. We therefore proceeded to investigate ERCC1 and PARP1 co-expression in ovarian cancer. As shown in supplementary Table S5, ERCC1+ and PARP1+ tumors were more likely to be serous cystadenocarcinomas ($p = 0.000007$), high grade ($p = 0.001$) with residual disease before chemotherapy ($p = 0.02$). Tumors with low ERCC1 and low PARP1 had better PFS ($p = 0.0001$) (Fig. 1F) and better OS ($p = 0.0002$) (Fig. 1G).

3.3. Multivariate analysis

ERCC1, XPF and PARP1 were investigated in a Cox multivariate model (Table 1). In the whole cohort, ERCC1 and platinum sensitivity was independently associated with PFS ($p = 0.002$ and $p < 0.0001$, respectively). In platinum sensitive group, ERCC1 remained independently associated with PFS ($p = 0.034$) but not in platinum resistant group.

3.4. ERCC1 mRNA expression and ovarian cancer

For additional validation at the transcript level, we investigated *ERCC1* mRNA expression in ovarian cancer patients who received platinum based chemotherapy. As expected, high *ERCC1* mRNA expression was associated with poor progression free survival ($p = 0.0048$)

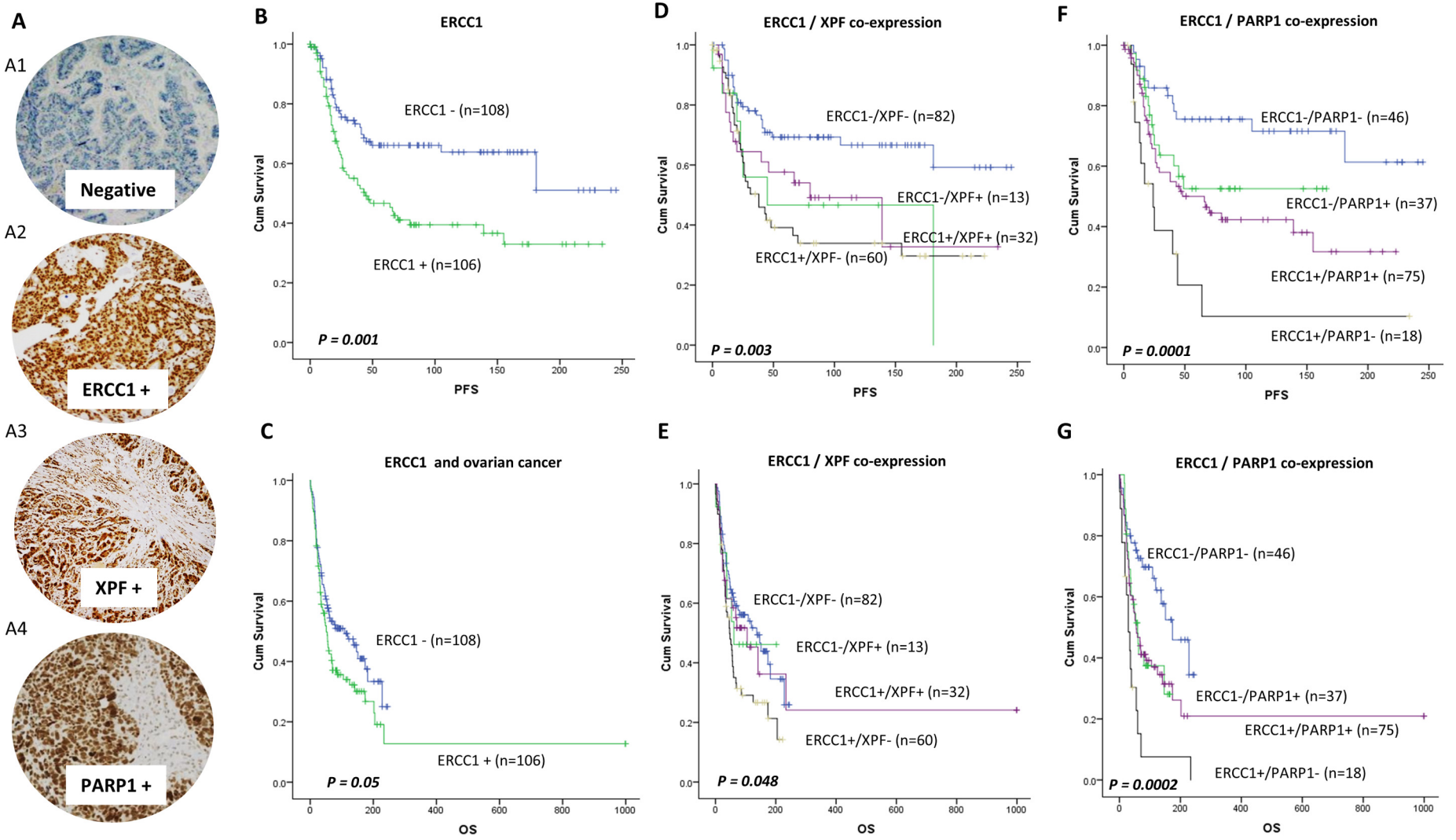

Fig. 1. A. Immunohistochemical (IHC) expression. Negative (A1), ERCC1+ (A2), XPF+ (A3) and PARP1+ (A4) in ovarian cancers. **B**. Kaplan-Meier curve for progression free survival (PFS) based on ERCC1 expression. **C**. Kaplan-Meier curve for overall survival (OS) based on ERCC1 expression **D**. Kaplan–Meier survival curves for PFS based on ERCC1-XPF co-expression. **E**. Kaplan–Meier survival curves for OS based on ERCC1-XPF co-expression. **F**. Kaplan–Meier survival curves for PFS based on ERCC1-PARP1 co-expression. **G**. Kaplan–Meier survival curves for OS based on ERCC1-PARP1 co-expression.

Table 1
Multivariate analysis for progression free survival in ovarian cancer.

Whole cohort				
	Sig.	Exp(B)	95.0% Confident interval	
			Lower	Upper
Platinum treatment	<**0.0001**	34.4	11.7	101.3
XPF	0.263	0.7	0.4	1.3
ERCC1	**0.002**	2.5	1.4	4.6
PARP1	0.887	0.9	0.5	1.7
Platinum sensitive group				
XPF	0.572	0.8	0.5	1.5
ERCC1	**0.034**	1.9	1.1	3.6
PARP1	0.641	1.2	0.6	2.2
Platinum resistant group				
XPF	0.434	0.4	0.1	3.5
ERCC1	0.550	0.5	0.1	4.3
PARP1	0.382	2.8	0.3	26.6

(Supplementary Fig. S1C) and poor overall survival ($p = 0.0006$) (Supplementary Fig. S1D).

Taken together the data provides evidence that high ERCC1expression is associated with poor outcome in the context of platinum treatment and therefore ERCC1 can be used as a predictor of platinum resistance in ovarian cancers.

3.5. Platinum sensitivity in ERCC1 or XPF deficient ovarian cancer cells

We initially screened a panel of ovarian cancer cell lines for ERCC1 and XPF expression. In whole cell lysates, as shown in Fig. 2A, A2780cis cells have significant high basal levels of XPF and higher ERCC1 levels compared to A2780 cell lines and other cell lines. A2780 is well described platinum sensitive ovarian cancer cell line established from a patient with previously untreated ovarian cancer and A2780cis is a platinum resistant cell line developed by chronic exposure of the parent cisplatin-sensitive A2780 cell line to increasing concentrations of cisplatin. In clonogenic assay we first confirmed platinum sensitivity or resistance in A2780 and A2780cis cells respectively (Fig. 2B). We then evaluated ERCC1 and XPF levels in nuclear and cytoplasmic extracts from A2780 and A2780cis cells before and after 24 h of cisplatin treatment (Fig. 2C1). In untreated samples, nuclear levels of ERCC1 and XPF were significantly higher in A2780cis compared to A2780 cells (Fig. 2C2). Whereas the cytoplasmic levels were lower in A2780cis compared to A2780 cells (Supplementary Fig. S2). Following 24 h of cisplatin, we observed a significant increase in ERCC1 nuclear level in A2780cis cells compared to A2780 cells (Fig. 2C2). No significant changes were observed in A2780 cells. We then depleted ERCC1 or XPF in A2780 as well as in A2780cis cells using siRNAs (Fig. 2D, Supplementary Fig. S3) and investigated platinum sensitivity. In platinum resistant A2780cis cells, ERCC1 depletion substantially increased platinum sensitivity (Fig. 3A). As A2780cis cells are p53 wild type (Supplementary Fig. S4), we also tested p53 mutant platinum resistant PEO4 cells. ERCC1 or XPF depletion (Fig. 2D3 and Supplementary Fig. S3) also substantially increased platinum sensitivity in PEO4 cells (Fig. 3E).

We then preceded to functional studies in A2780cis cells. Increased sensitization was associated with double strand break (DSB) accumulation (Fig. 3F), S-phase cell cycle arrest (Fig. 3G) and accumulation of apoptotic cells (Fig. 3H). In A2780 platinum sensitive cells, ERCC1 depletion lead to modest further sensitization (Fig. 3B), DSB accumulation (Fig. 3F), S-phase cell cycle arrest (Fig. 3G) and accumulation of apoptotic cells (Fig. 3H). XPF depletion resulted in platinum sensitization in A2780cis (Fig. 3C) and A2780 cells (Fig. 3D). Increased sensitization was associated with DSB accumulation (Fig. 3I) and apoptosis (Fig. 3K). S-phase arrest at 24 h and G1 arrest at 48 h was evident in both control and A2780_XPF depleted cells treated with cisplatin (Fig. 3J).

3.6. Olaparib is selectively toxic in ERCC1 or XPF deficient ovarian cancer cells

PARP1 inhibitors (olaparib, niraparib) are standard maintenance therapy to prolong PFS in platinum sensitive ovarian cancers [1,2]. A previous study in lung cancer models also suggested that PARP1 inhibition could be synthetically lethal in ERCC1 deficient cells. We therefore investigated if ERCC1 or XPF deficient ovarian cancer cells could be sensitive to Olaparib through synthetic lethality.

As expected, ERCC1 depletion significantly increased olaparib sensitivity (Fig. 4A, B), increased DSB accumulation (at 48 h) (Fig. 4F) compared to control and untreated cells. We observed significant G2/M cell cycle arrest in ERCC1 deficient A2780cis cells (Fig. 4G). Increased apoptotic cells were evident in ERCC1 depleted A2780cis and A2780 cells (Fig. 4H). Similar to ERCC1 data, XPF depletion also increased olaparib sensitivity (Fig. 4C and D). The increase in olaparib sensitivity was also confirmed in ERCC1 depleted or XPF depleted PEO4 platinum resistant cells (Fig. 4E). In A2780cis cells, increased sensitivity was associated with DSB accumulation (at 48 h) (Fig. 4I), G1-phase arrest (at 48 h) (Fig. 4J) and apoptosis (at 24 h) (Fig. 4K). In A2780 cells, similarly, there was S-phase arrest (Fig. 4J) and an increased apoptosis (Fig. 4K).

Taken together, the data provide evidence that ERCC1 or XPF depletion not only increases platinum sensitivity but also increased sensitivity to olaparib by synthetic lethality.

4. Discussion

ERCC1 is non-catalytic but partners with XPF endonuclease to form the ERCC1-XPF heterodimer which processes abnormal DNA repair intermediates generated during NER, DSB repair and ICL repair. ERCC1/XPF complex is associated with cisplatin resistance on some cancers [14,15]. In the current study, we have investigated ERCC1 and XPF expression in a large cohort of ovarian cancers and provided strong evidence that ERCC-XPF deficiency is a predictor of platinum sensitivity in patients. Pre-clinically, in platinum resistant ovarian cancer cells, ERCC1 and XPF expression is not only high in the nucleus but depletion of either ERCC1 or XPF substantially increased platinum sensitivity, with consequent accumulation on DNA DSBs, S-phase arrest and an increase in apoptosis. Depletion of ERCC1 in A2780cis cells (cisplatin-resistant), re-sensitized to platinum with sensitivity comparable to platinum sensitive A2780 ovarian cells. ERCC1 and XPF siRNA depletion was previously shown to increase cisplatin sensitivity in non-small lung [16] and breast cancer cells [17]. In a mouse xenograph model, ERCC1-deficient melanoma cells were also observed to be 10-fold more sensitive to cisplatin than ERCC1-proficient cells [18].

ERCC1 as a marker of platinum resistance has been well described in other solid tumors including lung, colorectal, head, neck, gastric and bladder cancers [19,20]. In ovarian cancers, a previous small study of 92 tumors showed that high ERCC1 was a marker of platinum resistance but no correlation with patient's survival was observed [21]. In another study of 101 ovarian cancer patients, high ERCC1 was linked to platinum resistance and reduced survival [22]. Taken together, including our study, the data suggest that high ERCC1 level is a predictor of platinum resistance. On the other hand, another study from two clinical trial cohorts, utilizing a polyclonal anti-ERCC1 antibody (FL297 clone), the investigators were unable to demonstrate the predictive influence of ERCC1 in ovarian cancers [23]. However, it should be noted that the use of a non-specific ERCC1 antibodies has been a major limitation in previous studies including in clinical trial cohorts [12]. In the current study we have utilised a recently generated and highly specific mouse monoclonal antibody (clone 4F9) [20] which strengthens our clinical data in ovarian cancer patients. The clinicopathological significance of

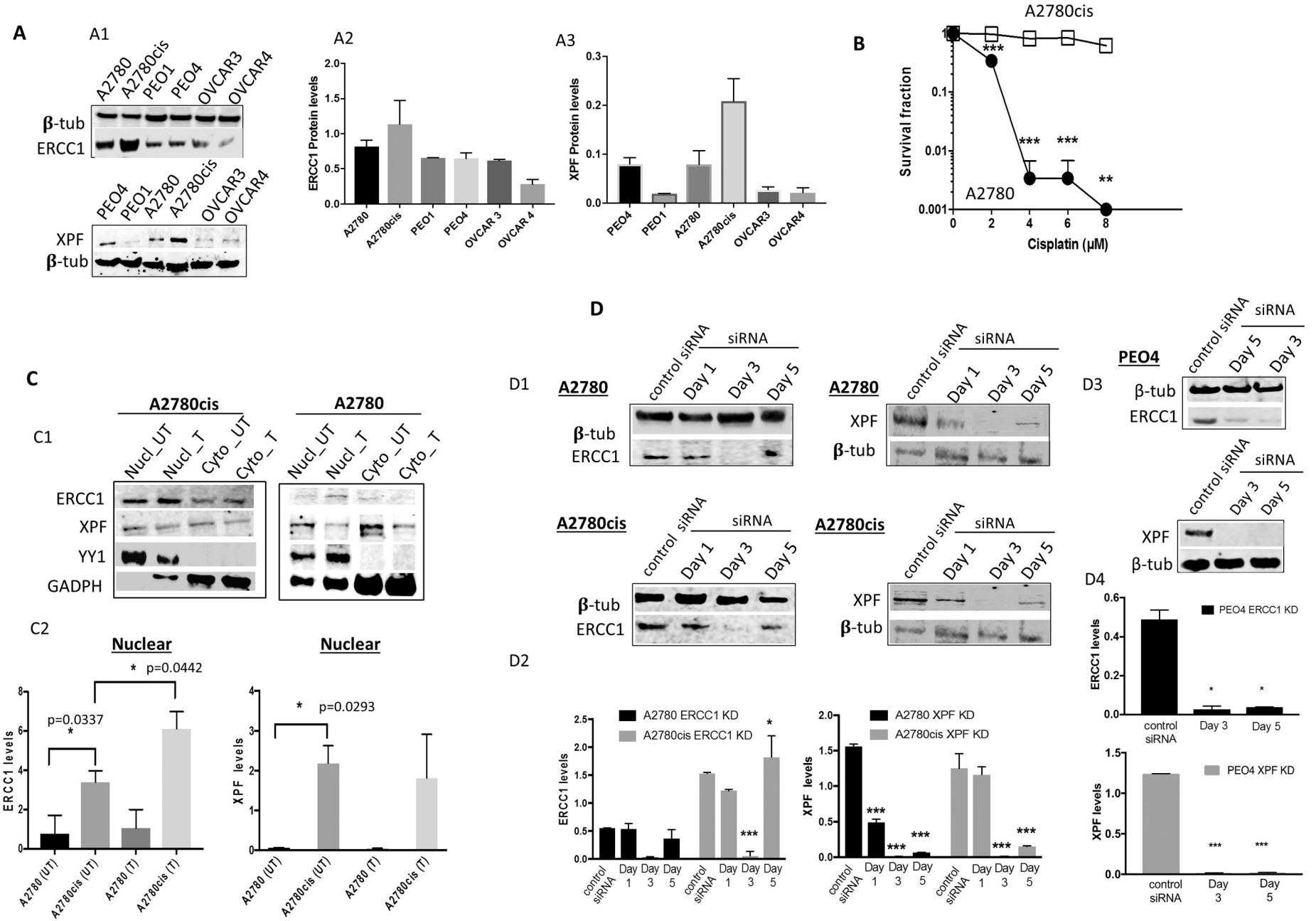

Fig. 2. **A**. ERCC1 (A1, A2) and XPF (A1, A3) levels in various ovarian cancer cell lines. β-Tubulin (β-tub) was used as a loading control. **B**. Clonogenic cell survival in cisplatin treated A2780 and A2780cis cells. **C**. Representative immunoblots of nuclear and cytoplasmic levels of ERCC1 and XPF (**C1**) in A2780 and A2780cis cells. Quantification of nuclear levels of ERCC1 and XPF are shown in **C2** (cytoplasmic levels of ERCC1 and XPF are shown in Supplementary Fig. S2). GADPH was used as a loading control for the cytoplasmic fractions and YY1 as a loading control to the nuclear fractions. **D**. Representative immunoblots of ERCC1 and XPF levels in A2780 (**D1**), A2780cis (**D1**) and PEO4 cells (**D3**) transfected with control siRNA or ERCC1/XPF siRNA. Quantification is summarized in **D2** and **D4**. β-Tubulin (β-tub) was used as a loading control. Data are means ± S.D. of three or more independent experiments.

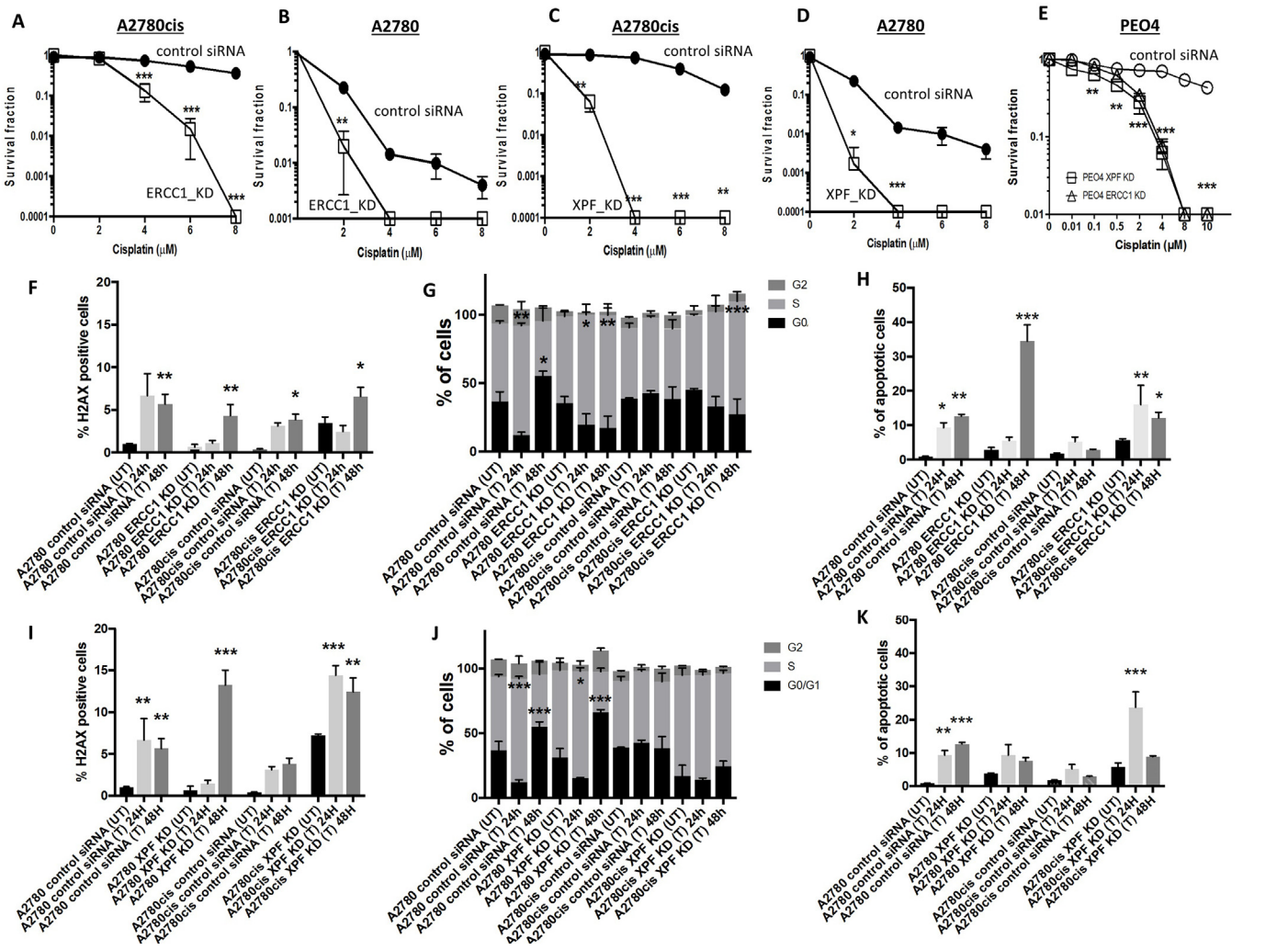

Fig. 3. A. Clonogenic cell survival in cisplatin treated A2780cis cells (control siRNA compared to ERCC1 siRNA transfected cells). **B**. Clonogenic cell survival in cisplatin treated A2780 cells (control siRNA compared to ERCC1 siRNA transfected cells). **C**. Clonogenic cell survival in cisplatin treated A2780cis cells (control siRNA compared to XPF siRNA transfected cells). **D**. Clonogenic cell survival in cisplatin treated A2780 cells (control siRNA compared to XPF siRNA transfected cells). **E**. Clonogenic cell survival in cisplatin treated PEO4 cells (control siRNA compared to XPF siRNA transfected cells or ERCC1 siRNA transfected cells). **F**. Percentage of γH2Ax-positive cells in untreated or cisplatin treated A2780 and A2780cis cells (control siRNA compared to ERCC1 siRNA transfected cells). **G**. Cell cycle analysis in untreated or cisplatin treated A2780 and A2780cis cells (control siRNA compared to ERCC1 siRNA transfected cells). **H**. Anexin V analysis by flow cytometry in untreated or cisplatin treated A2780 and A2780cis cells (control siRNA compared to ERCC1 siRNA transfected cells). **I**. Percentage of γH2Ax-positive cells in untreated or cisplatin treated A2780 and A2780cis cells (control siRNA compared to XPF siRNA transfected cells). **J**. Cell cycle analysis in untreated or cisplatin treated A2780 and A2780cis cells (control siRNA compared to XPF siRNA transfected cells). **K**. Anexin V analysis by flow cytometry in untreated or cisplatin treated A2780 and A2780cis cells (control siRNA compared to XPF siRNA transfected cells).Data are means ± S.D. of three or more independent experiments.

XPF in ovarian cancer has also not been described previously. Although no significance was observed between XPF expression and pathological features, tumors with low ERCC1/low XPF co-expression showed more favorable progression free survival implying platinum sensitivity.

In platinum sensitive disease, PARP1 inhibitor (Niraparib, Olaparib, Rucaparib) maintenance therapy was recently shown to substantially improve progression free survival [24–26]. In the current study, increased sensitivity to Olaparib treatment was shown in ERCC1 or XPF depleted A2780cis and PEO4 cells. Although increased sensitivity suggests a synthetic lethality relationship between PARP inhibition and ERCC1 or XPF deficiency, additional studies are required in other ERCC1/XPF deficient or knockout ovarian cancer cells. We have concluded increased sensitivity to Olaparib therapy for the following reasons; 1) ERCC1 or XPF deficient cells were sensitive to Olaparib treatment. 2) Functional analyses in ERCC1 or XPF deficient cells confirmed that Olaparib therapy led to an accumulation of DNA DSBs, cell cycle arrest and apoptotic cells. The data is consistent with pre-clinical studies of PARP inhibitors in ERCC1 deficient lung cancer models [12,13]. Previously, Horton et al. have demonstrated that PARP inhibitors are synthetically lethal in BER deficient cells [27]. More recently we have also confirmed that PARP inhibitors are synthetically lethal in XRCC1 deficient breast cancers [28]. Together the data, including ours, would imply that PARP inhibitors are likely to have additional applications in cancers.

We conclude that ERCC1-XPF deficiency is not only a predictor of platinum sensitivity but may also be a clinical tool to personalize Olaparib therapy in ovarian cancer patients. Further prospective studies are warranted to confirm our observation.

Supplementary data to this article can be found online at https://doi.org/10.1016/j.ygyno.2019.02.014.

Authors' contributions

Study design: KM and SM.

Data acquisition, interpretation and analyses: KM, MA, MG, MST, TMAA, PM, AA and SM.

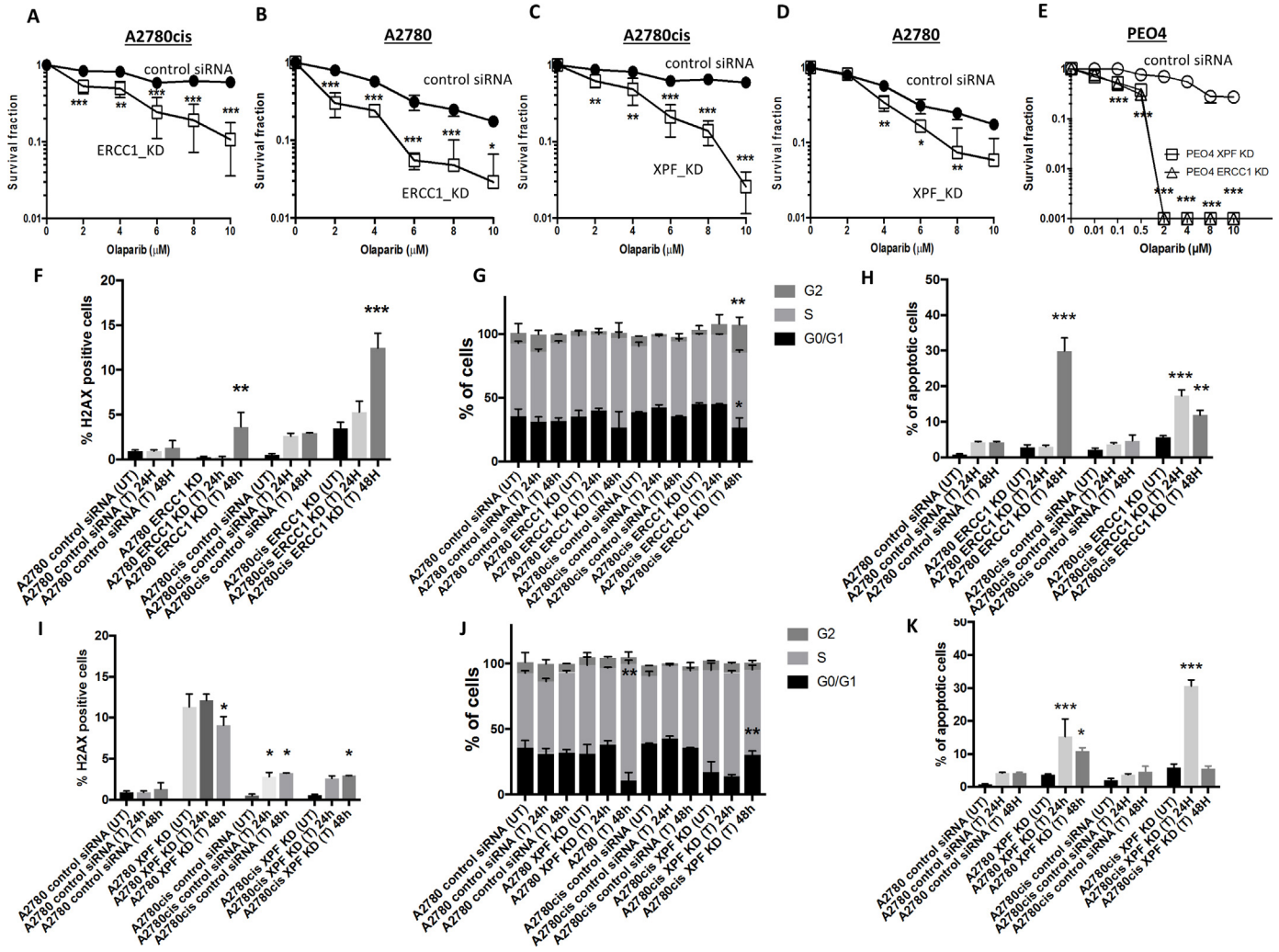

Fig. 4. A. Clonogenic cell survival in olaparib treated A2780cis cells (control siRNA compared to ERCC1 siRNA transfected cells). **B**. Clonogenic cell survival in olaparib treated A2780 cells (control siRNA compared to ERCC1 siRNA transfected cells). **C**. Clonogenic cell survival in olaparib treated A2780cis cells (control siRNA compared to XPF siRNA transfected cells). **D**. Clonogenic cell survival in olaparib treated A2780 cells (control siRNA compared to XPF siRNA transfected cells). **E**. Clonogenic cell survival in olaparib treated PEO4 cells (control siRNA compared to XPF siRNA transfected cells or ERCC1 siRNA transfected cells). **F**. Percentage of γH2Ax-positive cells in untreated or olaparib treated A2780 and A2780cis cells (control siRNA compared to ERCC1 siRNA transfected cells). **G**. Cell cycle analysis in untreated or olaparib treated A2780 and A2780cis cells (control siRNA compared to ERCC1 siRNA transfected cells). **H**. Anexin V analysis by flow cytometry in untreated or olaparib treated A2780 and A2780cis cells (control siRNA compared to ERCC1 siRNA transfected cells). **I**. Percentage of γH2Ax-positive cells in untreated or olaparib treated A2780 and A2780cis cells (control siRNA compared to XPF siRNA transfected cells). **J**. Cell cycle analysis in untreated or olaparib treated A2780 and A2780cis cells (control siRNA compared to XPF siRNA transfected cells). **K**. Anexin V analysis by flow cytometry in untreated or olaparib treated A2780 and A2780cis cells (control siRNA compared to XPF siRNA transfected cells). Data are means ± S.D. of three or more independent experiments.

Draft preparation, writing, review, editing of manuscript and approval of final manuscript: KM, MA, MG, MST, TMAA, PM, SYTC, EAR and SM.

Conflict of interest

The authors disclose no potential conflicts of interest.

References

[1] J. Ledermann, P. Harter, C. Gourley, M. Friedlander, I. Vergote, G. Rustin, et al., Olaparib maintenance therapy in platinum-sensitive relapsed ovarian cancer, N. Engl. J. Med. 366 (2012) 1382–1392.
[2] M.R. Mirza, B.J. Monk, J. Herrstedt, A.M. Oza, S. Mahner, A. Redondo, et al., Niraparib maintenance therapy in platinum-sensitive, recurrent ovarian cancer, N. Engl. J. Med. 375 (2016) 2154–2164.
[3] E.M. Swisher, K.K. Lin, A.M. Oza, C.L. Scott, H. Giordano, J. Sun, et al., Rucaparib in relapsed, platinum-sensitive high-grade ovarian carcinoma (ARIEL2 part 1): an international, multicentre, open-label, phase 2 trial, Lancet Oncol. 18 (2017) 75–87.
[4] C.-C.L. David Lopez-Martinez, A. Martin, Cohn. Cellular response to DNA interstrand crosslinks: the Fanconi anemia pathway, Cell. Mol. Life Sci. 73 (2017) 3097–3114.
[5] P. Spyridon, L.L. Basourakos, M. Ana, Aparicio et al. combination platinum-based and DNA damage response-targeting cancer therapy: evolution and future directions, Curr. Med. Chem. 24 (2017) 1586–1606.
[6] J.S. Jennifer Ma, Y. Nancy, Lee et al. the therapeutic significance of mutational signatures from DNA repair deficiency in cancer, Nat. Commun. 9 (2018) 3292.
[7] J.P.L. Vincent Mocquet, Thilo Riedl, et al., Sequential recruitment of the repair factors during NER: the role of XPG in initiating the resynthesis step, EMBO J. 27 (2007).
[8] R. George, Simon RI-KaG, Nuclear excision repair-based personalized therapy for non-small cell lung cancer: from hypothesis to reality, Int. J. Biochem. Cell Biol. 39 (2017) 1318–1328.
[9] MFaLH Mullenders, Transcription-coupled nucleotide excision repair in mammalian cells: molecular mechanisms and biological effects, Cell Res. 18 (2008) 73–84.
[10] Isao Kuraoka WRK, Rafael R. Ariza, et al., Repair of an interstrand DNA cross-link initiated by ERCC1-XPF repair/recombination nuclease, J. Biol. Chem. 275 (2000) 26632–26636.
[11] O.D.S. Cheryl Clauson, Laura Niedernhofer, Advances in understanding the complex mechanisms of DNA interstrand cross-link repair, Cold Spring Harb. Perspect. Biol. 5 (2013), a012732. .
[12] S.B.I. Postel-Vinay, L. Friboulet, et al., A high-throughput screen identifies PARP1/2 inhibitors as a potential therapy for ERCC1-deficient non-small cell lung cancer, Oncogene 32 (2013) 5377–5387.
[13] H. Cheng, Z. Zhang, A. Borczuk, C.A. Powell, A.S. Balajee, H.B. Lieberman, et al., PARP inhibition selectively increases sensitivity to cisplatin in ERCC1-low non-small cell lung cancer cells, Carcinogenesis 34 (2013) 739–749.

[14] S.P.-S.A. Usanova, U. Sied, J. Thomale, et al., Cisplatin sensitivity of testis tumour cells is due to deficiency in interstrand-crosslink repair and low ERCC1-XPF expression, Mol. Cancer 9 (2010) 248.
[15] E.M.M.D. McNeil, DNA repair endonuclease ERCC1-XPF as a novel therapeutic target to overcome chemoresistance in cancer therapy, Nucleic Acids Res. 40 (2012) 9990–10004.
[16] S.K.A. Arora, K. Tillison, V. Kalman-Maltese, et al., Downregulation of XPF-ERCC1 enhances cisplatin efficacy in cancer cells, DNA Repair (Amst) 9 (2010) 745–753.
[17] I.Y.K.M. Chang, H.B. Kim, D.Y. Lee, et al., Small interfering RNA-induced suppression of ERCC1 enhances sensitivity of human cancer cells to cisplatin, Biochem. Biophys. Res. Commun. 327 (2005) 225–233.
[18] R.A. Song L1, E.M. McNeil, Identification of DNA repair gene Ercc1 as a novel target in melanoma, Pigment Cell Melanoma Res. 24 (2011) 966–971.
[19] George D. Cimino, C-xPaPTH, Personalized medicine for targeted and platinum-based chemotherapy of lung and bladder cancer, Bioanalysis 5 (2013) 369–391.
[20] B.N.G.F. Bahamon, H. Danaee, Development and validation of an ERCC1 immunohistochemistry assay for solid tumors, Arch. Pathol. Lab. Med. 140 (2016) 1397–1403.
[21] P.W.Y. Du, L. Chen, Y. Gan, Q. Wu, High ERCC1 expression is associated with platinum-resistance, but not survival in patients with epithelial ovarian cancer, Oncol. Lett. (2016) 12.
[22] K.D. Steffensen, WMaJA, The relationship of platinum resistance and ERCC1 protein expression in epithelial ovarian cancer, Int. J. Gynecol. Cancer 19 (2009) 820–825.
[23] Jennifer M. Rubatt, KMD, Chunqiao Tian, et al., Pre-treatment tumor expression of ERCC1 in women with advanced stage epithelial ovarian cancer is not predictive of clinical outcomes, Gynecol. Oncol. 125 (2012) 421–426.
[24] MSaD Edessa, PARP inhibitors as potential therapeutic agents for various cancers: focus on niraparib and its first global approval for maintenance therapy of gynecologic cancers, Gynecol. Oncol. Res. Pract. 4 (2017) 18.
[25] O.A.C. Dizdar, K. Altundag, Advances in PARP inhibitors for the treatment of breast cancer, Expert. Opin. Pharmacother. 16 (2015) 2751–2758.
[26] N.J.S.C. Curtin, Therapeutic applications of PARP inhibitors: anticancer therapy and beyond, Mol. Asp. Med. 34 (2013) 1217–1256.
[27] J.K. Horton, D.F. Stefanick, R. Prasad, N.R. Gassman, P.S. Kedar, S.H. Wilson, Base excision repair defects invoke hypersensitivity to PARP inhibition, Mol. Cancer Res. 12 (2014) 1128–1139.
[28] R. Ali, A. Al-Kawaz, M.S. Toss, A.R. Green, I.M. Miligy, K.A. Mesquita, et al., Targeting PARP1 in XRCC1 deficient sporadic invasive breast cancer or pre-invasive ductal carcinoma in situ induces synthetic lethality and chemoprevention, Cancer Res. 78 (24) (2018) 6818–6827.